

DETERMINATION OF TRAIN SPEED LIMITS ON RENEWED TRACKS USING TAMPING MACHINE AND NUMERICAL OPTIMISATION

V.L. Markine, C. Esveld

Section of Road and Railway Engineering
Faculty of Civil Engineering, Delft University of Technology
Stevinweg 1, NL-2628, CN Delft, The Netherlands
E-mail: v.l.markine@citg.tudelft.nl, c.esveld@citg.tudelft.nl

ABSTRACT

The paper presents a methodology for analysis of lateral resistance of a railway track and its application to determination of train speed limits for newly laid tracks or tracks after renewal. Ballast parameters and safe speed limits of trains are determined using the same 3-D finite element model. First, the model parameters related to the lateral resistance of ballast are determined on the basis of measurement data. Lateral track load/displacements diagrams have been obtained by shifting a real track using a tamping machine (which is normally used to lift a track). The measurements are also simulated using the 3-D FE model of the track. Based on the experimental data and the results of numerical simulation, ballast parameters are determined using an optimisation technique (a Sequential Quadratic Programming method).

The track model with the obtained ballast parameters is then used to determine maximum allowable temperatures for typical train velocities according to safety criteria given in UIC Leaflet 720. Finally, by comparing the maximum allowable temperatures with combined equivalent ones, safe train speed limits are determined. The presented procedure is applied to determine speed limits for a railway track using track lateral resistance data measured at different moments after track renovation. The results are presented and discussed.

INTRODUCTION

Sufficient lateral strength of a railway track is important for safe track operations. High lateral forces acting on a track are caused by a moving train as well as by temperature variation. The lateral strength of a railway track is to a large extent defined by ballast lateral resistance. For a newly laid track or a track after full maintenance, ballast particles are not good enough consolidated and therefore lateral resistance of such a track is poor. This can be observed from Figure 1 where a typical lateral behaviour of well-consolidated and tamped ballast during a single sleeper test is shown. The peak strength F_p of tamped ballast is substantially lower than the one of consolidated ballast. In order to prevent track buckling, the lateral

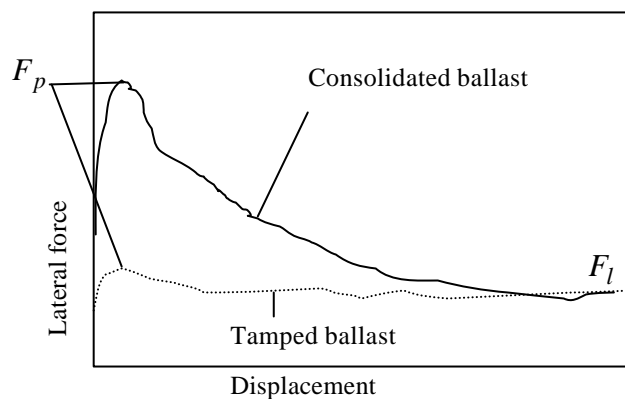


**Figure 1 Lateral behaviour of ballast in a single sleeper test
(not to scale)**

forces occurring during operations on newly laid tracks or tracks after maintenance should be restricted. Usually, this is achieved by temporary restriction of train speeds on renewed sections of such a track. As the number of train passes grows, ballast becomes more consolidated and its lateral resistance increases. Accordingly, the restriction of the speed limits can be released.

Obviously, an introduction of temporary speed restrictions deteriorates operational efficiency of a railway track. One way to reduce the operational hindrance is to use dynamic stabilisation directly after track maintenance. Yet, it is still necessary to know whether the imposed speed limitations are safe or not. To apply proper speed limits, knowledge about lateral resistance of a track and its interpretation for determination of safe speed limits are required [8].

In practice the lateral resistance of a track is measured using tamping machines. A tamping machine, which is normally used to lift up a track, shifts a track in the lateral direction. Lateral track resistance can then be determined from load/displacements diagrams obtained during measurements. Although such information could be used for estimation of ballast condition, it was not possible to directly use it for assignment of temporary speed limits for renewed tracks. On the other hand, UIC Leaflet 720 [6] gives safety criteria for tracks with continuously welded rails based on a rail temperature. Using these criteria it is possible to determine maximum allowable rail temperatures with no risk of buckling. The temperatures are obtained using a finite element model, which requires knowledge about lateral resistance of ballast. That is why, at Delft University of Technology a technique for identification of ballast lateral resistance parameters basing on measured lateral resistance of a real track has been developed, so that the UIC safety criteria could be applied for determination of temporary speed limits [8].

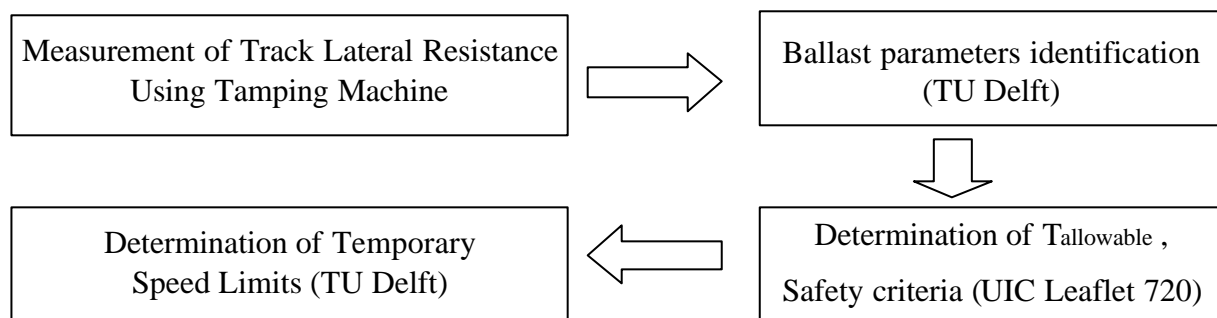


Figure 2 Flowchart of procedure for determination of temporary speed limits on renewed tracks

In this paper a technique developed at Delft University of Technology that provides a link between measurement of lateral resistance of a track and assignment of operational train speeds is presented (Figure 2). The 3-D finite element model of a railway track is used for both identification of ballast lateral resistance parameters and determination of the corresponding speed limits. Ballast resistance parameters are determined using load/displacements diagrams obtained by shifting a real track in the lateral direction. The field measurements are simulated using the finite element model of a track. Ballast resistance parameters are then determined by matching the results of the numerical simulation with measurement data. The identification of ballast parameters is performed using a modern optimisation technique.

The obtained ballast parameters are then used in the numerical model of a track for determination of train speed limits. The speed limits are determined by comparing the maximum allowable temperatures calculated according to the UIC safety criteria for a number of typical train speeds with combined equivalent ones. Both procedures (ballast parameter identification and determination

of speed limits) have been implemented in a software package BLATRES (TU Delft). Finally, the technique has been applied to determine train speed limits on a track after full maintenance.

NUMERICAL MODEL OF TRACK

The 3-D Finite Element (FE) model of a railway track used here is shown in Figure 3. The model can be used for analysis of both straight and curved tracks [8,14]. It also accounts for geometry misalignments which are approximated by a sine function (Figure 3a). Rails are modelled by 3-D elastic beam elements whereas for fasteners and ballast, linear as well non-linear spring elements are used. The choice between linear and non-linear spring elements was based on the experimental data of various tracks available from the literature [4,5,13,14]. Thus, the vertical behaviour of the ballast is described by linear spring elements (Figure 3b), which provide a support to rails also known as Winkler foundation [7]. A contribution of fastenings and ballast to the longitudinal resistance of a track is assumed to be linear and therefore they are also modelled using linear spring elements representing the total longitudinal stiffness of a track (Figure 3b). Combined torsional stiffness of a track which depends on a fastening system, track gauge and sleeper spacing, is approximated here by linear torsional springs (Figure 3a).

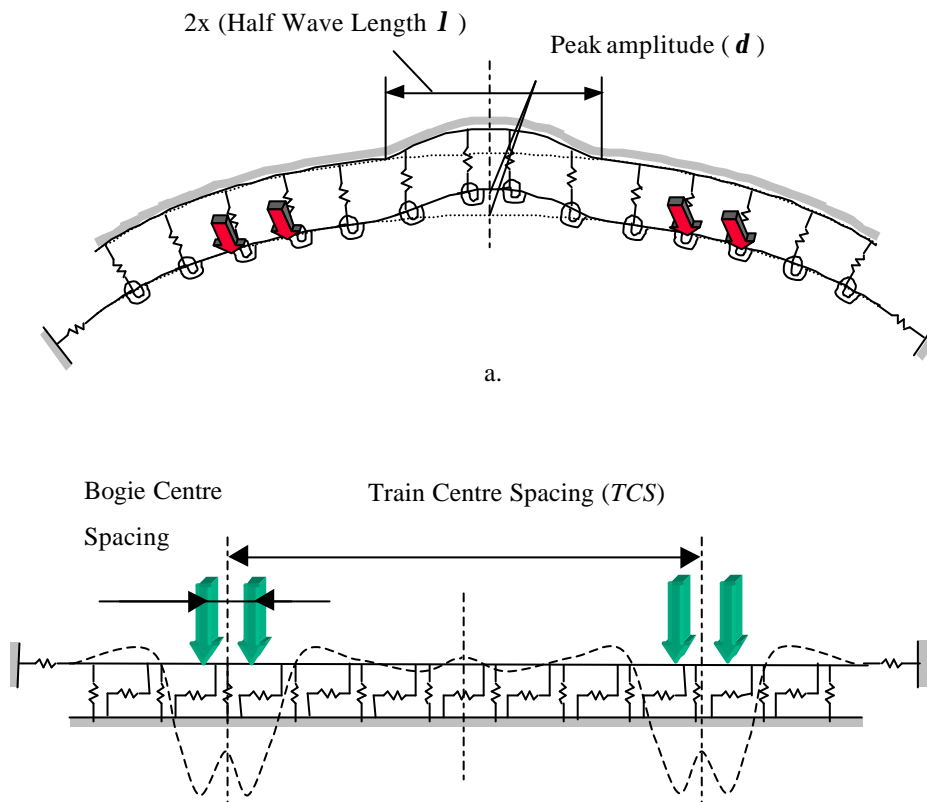


Figure 3 FE model of track: a. Top view; b. Side view

It is known from experiments (e.g. from a single sleeper test [14]) that the lateral behaviour of ballast is non-linear (Figure 1) to model which an elasto-plastic spring element is used. The element can describe two types of non-linear behaviour, namely bi-linear or non-linear with softening as shown in Figure 4. The element behaves as linear-elastic until the applied lateral load s has reached the peak value $s = F_p$ (in case of no vertical loads) and corresponding peak displacement W_p . After that the element begins to yield, that is the deformations are increasing with no increase of the force

s approaching its limit value F_l as shown in Figure 4. The stiffness K_{el} of the spring during the elastic stage is

$$K_{el} = \frac{F_p}{W_p} \quad (1)$$

The softening branch is described by the function

$$s = F_l + (F_p - F_l) 2^{-w/W_l} \quad (2)$$

The rate of softening is defined by the limit value of the parameter $W_l > W_p$ so that the force s corresponding to the displacement $w = W_l$ is equal to the average between F_p and F_l (Figure 4a). From (2) it can be seen that if the limit strength F_l is taken equal to the peak strength F_p the model describes bi-linear ballast behaviour as shown in Figure 4b.

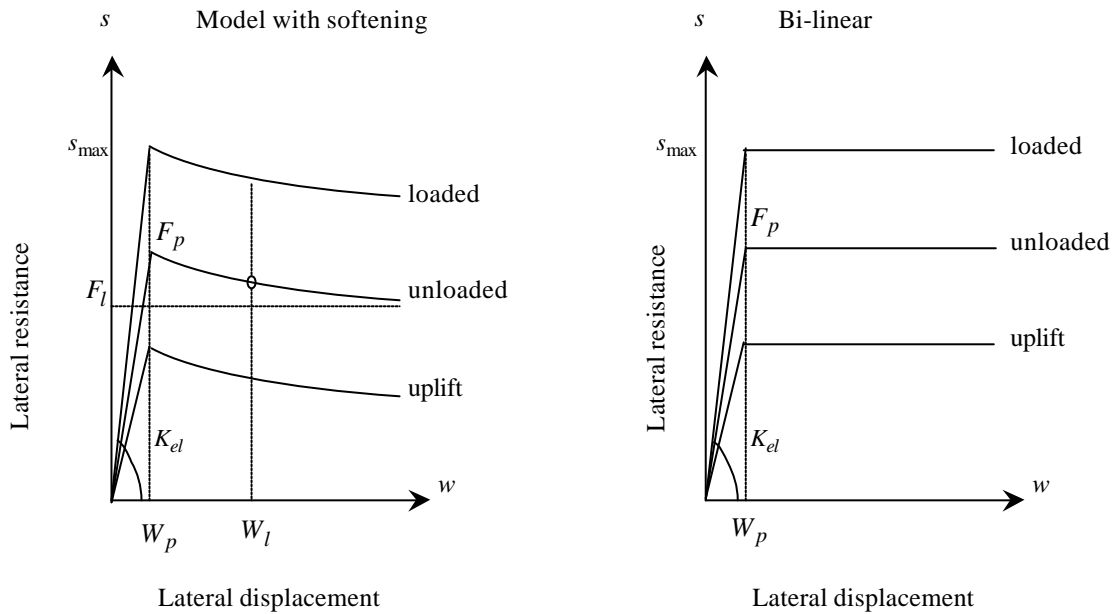


Figure 4 Lateral ballast behaviour (model): a. with softening; b. bi-linear

From experimental data it is known that ballast behaviour depends on vertical loads. The model accounts for the effect of vertical forces by introducing the Mohr-Coulomb criterion. The yielding now occurs at the force s_{max} (loaded and uplift branches on Figure 4) which is evaluated as

$$s_{max} = F_p - s_v \tan \mathbf{j} \quad (3)$$

where

F_p is the peak strength of ballast for unloaded track;

s_v is the vertical load per unit length;

$\tan \mathbf{j}$ is the friction coefficient between the sleeper and ballast. Thus, if no vertical load is applied, ($s_v = 0$), the ballast yields at the lateral force $s_{max} = F_p$.

The stiffness of ballast K_{el} also depends on the vertical load and can be obtained from (1) and (3) according to the formula

$$K_{el} = \frac{F_p - s_v \tan j}{W_p} \quad (4)$$

where W_p is the peak elastic displacement for unloaded track (reference case). To approximate the softening branch one can notice that in case of loading the peak strength of the ballast is changing by the factor $b = s_{\max} / F_p$. Assuming linear dependence of the lateral resistance from vertical

loads, the ballast limit strength F_l is also increased by the factor b and becomes equal to $F_l \frac{s_{\max}}{F_p}$.

Introducing the parameter $s_{\lim} = F_l / F_p$ and taking into account (2) the softening branch in presence of vertical load can be described by the formula

$$s = s_{\max} [s_{\lim} + (1 - s_{\lim}) 2^{-w/W_l}] \quad (5)$$

Thus, the bi-linear ballast model is characterised by the two elastic parameters F_p , W_p and the friction coefficient $\tan j$ whereas the model with softening is defined by five parameters, namely F_p , F_l , W_p , W_l and $\tan j$. The model with softening can accurately describe ballast behaviour but its use requires a non-linear static response analysis, which can be time consuming. On the other hand, the response quantities of a track can be obtained very fast if a bi-linear model of ballast is used, since the response analysis in this case is linear.

An example of simulation of the lateral behaviour of a track using bi-linear ballast model is given in Figure 5 a. In this example, a track is loaded by the lateral force that uniformly increases from 0 to 17 kN. Additionally, the vertical load $F_v = 100 \text{ kN}$ has been applied to the track (the same application point as the lateral load). The simulated lateral displacements of the track plotted for the load application point are shown in Figure 5 b. The corresponding ballast behaviour in the lateral direction (bi-linear model) is shown in Figure 5 a. From these figures it can be observed that plastic deformations of the track \bar{W}_p occur when the yielding of ballast (W_p) begins, i.e.

$$\bar{W}_p = W_p = 2 \text{ mm} \quad (6)$$

Thus, the lateral behaviour of a railway track can be simulated using the above described numerical model providing that ballast lateral resistance is known. On the other hand, if the lateral resistance of a whole track is known one can try to solve an inverse problem to determine the parameters defining the lateral behaviour of ballast. A procedure for determination of ballast parameters using an optimisation technique is presented below.

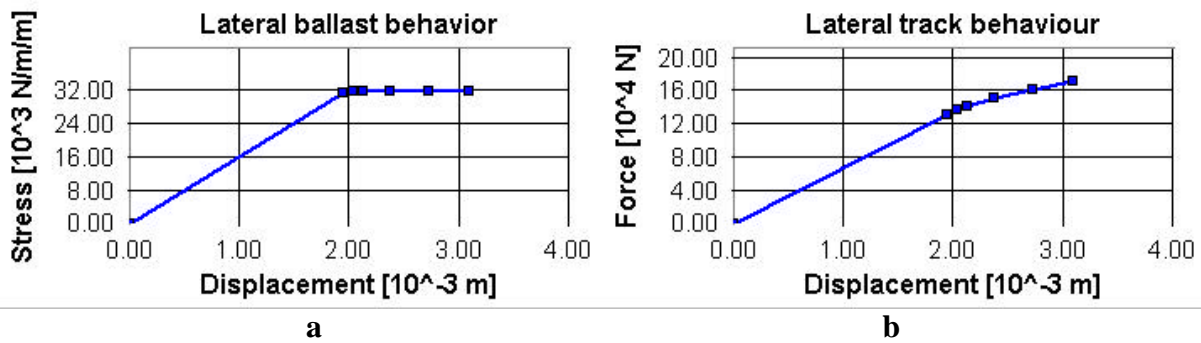


Figure 5 Lateral behaviour of ballast (a) and whole track (b)

DETERMINATION OF BALLAST LATERAL RESISTANCE

Lateral resistance of ballast can be estimated by performing a test with a separate sleeper or a track panel [15]. However, it can be very expensive or even impossible. In this section a procedure for extracting of the ballast characteristics from total lateral resistance of a track is presented.

Measurement of lateral resistance of track

One technique for measurement of lateral resistance of a track employed by Nederlandse Spoorwegen (Netherlands Railway) is presented here. The technique makes use of a tamping machine, which, instead of lifting, shifts a track frame in the lateral direction. To amplify the effect of vertical loads on the lateral resistance of a track, an additional vertical load can be applied as well. The resulting lateral displacements of the frame are measured and recorded. The applied lateral force and resulting lateral displacements of the track are then combined in a force-displacement diagram.

A typical force-displacement diagram is shown in Figure 6. An applied lateral force is slowly increased that results in movement of a track frame (path O-A in Figure 6). As the lateral displacements have achieved a prescribed maximum value (point B in Figure 6) shifting grips are released so that the track frame is moving back (path B-C-D in Figure 6). It should be noted that the maximum displacements of the track during the test are relatively small (max. 5mm) so that the residual displacements of the track are not very large and the original track geometry can easily be restored. The elastic characteristics of the track can be obtained by considering the residual displacements of the track (path O-D in Figure 6).

The maximum elastic displacements \bar{W}_p^{ex} of the track are then estimated by the displacements of the track Δ after the lateral load has been released (path B-C-D in Figure 6), i.e.

$$\bar{W}_p^{ex} = \Delta. \quad (7)$$

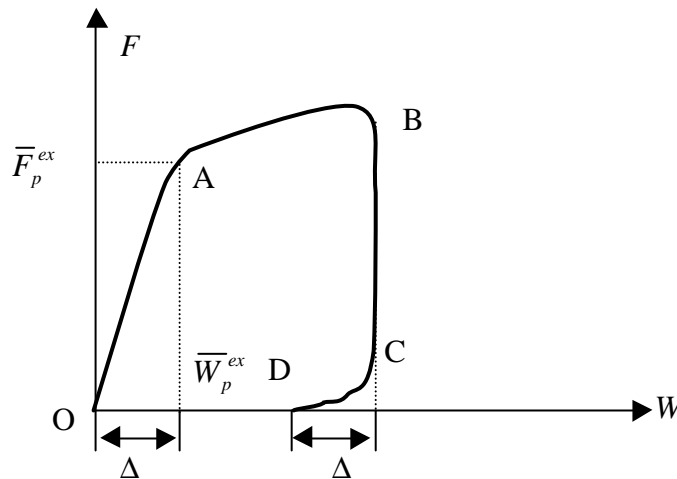


Figure 6 Force-displacement diagram of track measured employing tamping machine

The maximum elastic force \bar{F}_p^{ex} can be obtained from the force-displacement diagram as well. The elastic properties of the track machine \bar{F}_p^{ex} and \bar{W}_p^{ex} measured employing a tamping will be used here for ballast parameter identification.

BALLAST PARAMETER IDENTIFICATION

General parameter identification problem

In typical parameter identification problem there is an object (or process) to be investigated and there is a numerical model that can describe behaviour of such an object. The investigated object is considered as a black box that produces responses depending on values of some input parameters X . The numerical model is characterised by the object parameters X as well as by several tuning parameters $\mathbf{a} = [a_1, \dots, a_N]^T$. The goal of the identification problem is to find a set of the parameters \mathbf{a} such that the obtained numerical model most accurately describes the object behaviour, in other words the difference between the object and model responses for the same set of input parameters should be minimal. Thus, a general parameter identification problem can be formulated as the following minimization problem:

Minimize

$$G(\mathbf{a}) \equiv \sum_{p=1}^P |\mathbf{F}(X_p) - \tilde{\mathbf{F}}(X_p, \mathbf{a})| \quad (8)$$

subject to the constraints

$$A_i \leq a_i \leq B_i, \quad i = 1, \dots, N \quad (9)$$

where

$\mathbf{a} = [a_1, \dots, a_N]^T$ is the vector of the design variables (tuning parameters of the numerical model) that can be varied during the optimization;

\mathbf{F} is a set of responses obtained from experiments with the object;

$\tilde{\mathbf{F}}$ is a set of responses of the numerical model;

A_i, B_i are the upper and lower bound of the tuning parameter a_i ;

X_p is the p -th set of input parameters of the original object;

P is the total number of such sets.

A solution of the problem (8)-(9) \mathbf{a}^* can be found using a conventional method of mathematical programming. Here an optimisation technique based on a Sequential Quadratic Programming (SQP) method is used [9]. The method is iterative. It is based on successive linearizations of P non-linear differences in (8), combining a first order trust region method with a local method which uses approximate second order information. The first order derivatives are approximated by finite differences.

Identification of ballast parameters

The method for model parameter identification described above has been used for determination of ballast parameters F_p, W_p, F_l, W_l and $\tan \mathbf{j}$. Since the parameter characterising the elastic properties of the ballast (F_p and W_p) do not affect the plastic behaviour of a track and to speed up

an optimisation process, the parameters F_p and W_p can be determined separately from the other parameters. Moreover, due to a small shift of a track during measurements and therefore lack of experimental data about plastic deformations of a track it is difficult to obtain the values of the parameters F_l , W_l which characterise the plastic behaviour of ballast. That is why determination of these parameters is not discussed here although if the experimental data is available the same technique (as for the elastic parameters F_p and W_p) can be applied to determine the parameters F_l and W_l .

Using the methodology of the previous subsection one can try to find values of the ballast parameters F_p and W_p such that the displacement of a track in a reference point of the model \bar{W}_p and of a real track \bar{W}_p^{ex} due to the elastic limit force \bar{F}_p^{ex} are close as much as possible. Thus, the following optimisation problem similar to the problem (8)-(9) is to be solved

Minimise

$$G(\mathbf{a}) \equiv |\mathbf{F}(\mathbf{X}) - \tilde{\mathbf{F}}(\mathbf{X}, \mathbf{a})| \quad (10)$$

with

$$\mathbf{a} = [F_p \ W_p]^T, \mathbf{X} = [\bar{F}_p^{ex}], \mathbf{F}(\mathbf{X}) = [\bar{W}_p^{ex}], \tilde{\mathbf{F}}(\mathbf{X}) = [\bar{W}_p]. \quad (11)$$

Here the vector of the responses of the track structure \mathbf{F} (and consequently of the model $\tilde{\mathbf{F}}$) consists of the displacement only one point on the track \bar{W}_p^{ex} (and model displacement \bar{W}_p), namely the application point of the lateral force. If displacements of other points of a track are available they can be taken into account as well. Because of the linear relation between the force and displacement of the track, the displacements corresponding to one loading step $s = \bar{F}_p^{ex}$ are considered (i.e. $P=1$ in (8)). When non-linear behaviour of a track is analysed, more loading steps (components of the vector \mathbf{X}) should be used.

Since the track displacements are obtained performing a static linear analysis the optimisation problem(10)-(11) can be solved relatively fast. To speed up the optimisation it can also be assumed that yielding of the whole track occurs when ballast begins yield, i.e. $W_p = \bar{W}_p = \bar{W}_p^{ex}$. The vector of the design variables of the problem (10)-(11) then has only one component, namely $\mathbf{a} = [F_p]^T$.

If no extra vertical load is applied, the obtained optimal parameters $\mathbf{a}^* = [F_p^* \ W_p^*]^T$ are the elastic limits of ballast, i.e. $F_p = F_p^*$ and $W_p = W_p^*$. In case the measurement data have been obtained with extra vertical load F_v the obtained optimal parameter F_p^* is considered as the maximum yielding force $s_{max} = F_p^*$ defined in (3). The peak strength of ballast can then be calculated from (3) that reads

$$F_p = F_p^* + s_v \tan \mathbf{j} \quad (12)$$

where s_v is the vertical load per spring element. The corresponding limit deformation W_p

is evaluated as follows

$$W_p = \frac{F_p}{K_{el}}, \quad K_{el} = \frac{F_p^*}{W_p^*} \quad (13)$$

It should be noted that the rail temperature during the measurements can also be taken into account in the ballast parameter identification problem.

DETERMINATION OF SPEED LIMITS

As the ballast parameters have been obtained they can be used in the numerical model to determine maximum allowable speed limits. The calculation of speed limits is based on the safety criteria given in UIC Leaflet-720 [6]. According to these criteria, the maximum allowable temperature of the rails T_{allow} is defined by two critical buckling temperatures $T_{b,min}$ and $T_{b,max}$ (Figure 7) as follows

$$\text{if } \Delta T > 20^\circ\text{C}, \quad T_{allow} = T_{b,min} + 0.25\Delta T,$$

$$\text{if } 5^\circ\text{C} < \Delta T < 20^\circ\text{C}, \quad T_{allow} = T_{b,min},$$

$$\text{if } \Delta T \leq 0^\circ\text{C}, \quad T_{allow} = T_{b,min} - 5^\circ\text{C},$$

$$\text{where } \Delta T = T_{b,max} - T_{b,min}.$$

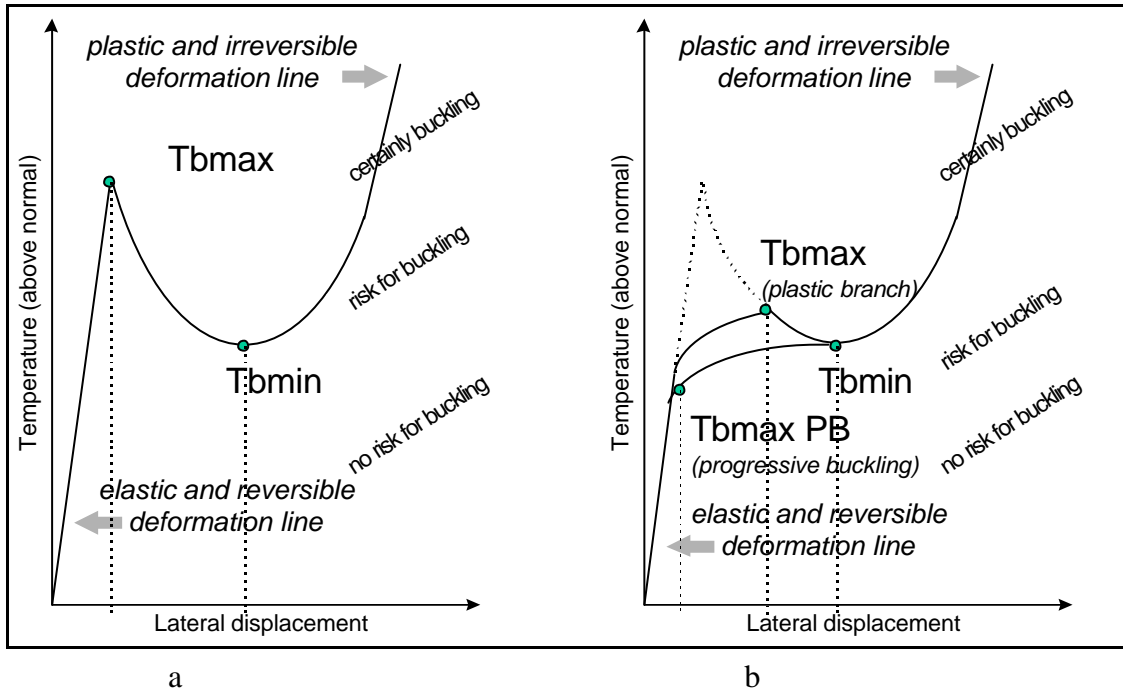


Figure 7 Critical buckling temperatures of rails

The critical buckling temperatures depend on a number of loading factors, namely the temperature loads, vertical train axle loads and lateral loads due to curvature of track and rail misalignments. The lateral forces depending on the train velocity, size of the misalignment and wheel quality are approximated here by the formula

$$F_{lat} = \frac{aMV^2}{R}, \quad (14)$$

where

V is the train velocity;

$R = \frac{2p^2d}{(2I)^2}$ is the equivalent radius of misalignments (Figure 3);

\mathbf{a} is a coefficient characterising wheel quality, viz. $\mathbf{a} = 1.0$ for a passenger train and $\mathbf{a} = 1.5$ for a freight train.

The track model (Figure 3) is used to calculate the maximum allowable temperature T_{allow} according to the safety criteria given above. Obviously, the track structure with no lateral load corresponding to the train velocity $V = 0 \text{ km/h}$ gives the maximum value of T_{allow} whereas calculations for higher train velocities result in lower temperatures T_{allow} . The maximum allowable temperatures $(T_{allow})_i, i = 1, \dots, N$ calculated for N typical velocities of the train are to be compared with a combined equivalent temperature T_{equiv} [6]. The combined temperature T_{equiv} depends on the following factors:

- actual track temperature relative to neutral temperature;
- effects of (eddy current) braking/accelerating;
- interaction with civil structures;
- etc.

The particular velocity of a train V_i is considered to be safe if the difference $T_{allow}|_{V_i} - T_{equiv}$ is positive. The maximum train velocity V^* for which the difference $T_{allow}|_{V^*} - T_{equiv}$ is still positive can be used as the train speed limit on a given track.

NUMERICAL EXAMPLE

Verification of parameter identification procedure

To verify the parameter identification procedure experimental data measured on a ballast track with wooden sleepers have been used [10]. The data has been obtained employing tamping machines. An average value of the measured maximum elastic lateral force and displacement of the track \bar{F}_p^{ex} and \bar{W}_p^{ex} (Figure 6) have been chosen as input values of the identification model (Table 1). A zero temperature of the rails during the experiment was chosen and the friction coefficient for the wooden sleepers $j = 1.1$ have been used. Other parameters of the model, which have been used to determine ballast parameters, can be found in [8].

Since there was no extra vertical load applied to the track structure during the measurements ($F_v = s_v = 0 \text{ N}$), the values of the parameters F_p^* and W_p^* obtained during the identification have been taken as ballast properties (see Eq. (12)), viz. $F_p = F_p^* = 44680 \text{ N/m}$, $W_p = W_p^* = 0.0018 \text{ m}$ (Table 1).

Input			Output			
$\bar{F}_p^{ex} [N]$	$\bar{W}_p^{ex} [m]$	T_{exp}	$F_p' [N/m/m']$	$F_p [N/m]$	$W_p [m]$	$K_{el} [N/m/m]$
64800	0.0018	0	12471	44680	0.0018	6928333

Table 1 Results of identification problem during verification

Ballast (spring element) and track lateral behaviour using the obtained ballast parameters when no extra vertical load is applied are shown in Figure 8.

To verify the results of identification, lateral resistance data of the same track measured with an extra vertical load $F_v = 100kN$ (applied at the application point of the lateral force [10]) have been used. The measurements with the extra vertical load have been simulated using the model with the obtained ballast parameters F_p and W_p . The results of the simulation are shown in Figure 9.

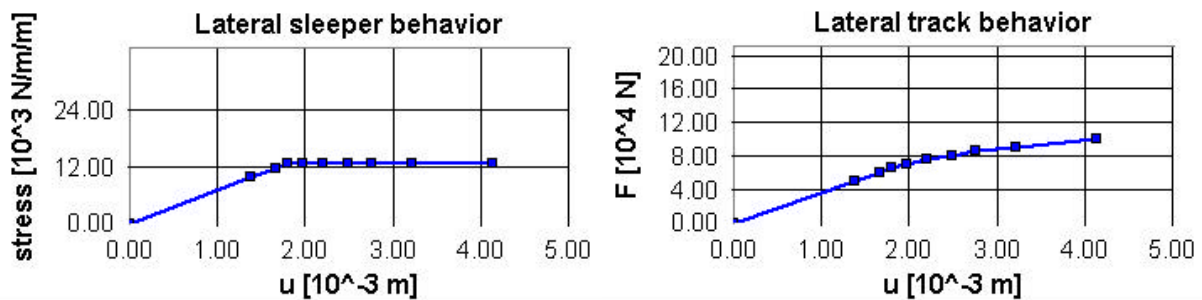


Figure 8 Model obtained using measurement data without vertical load; case with no vertical load

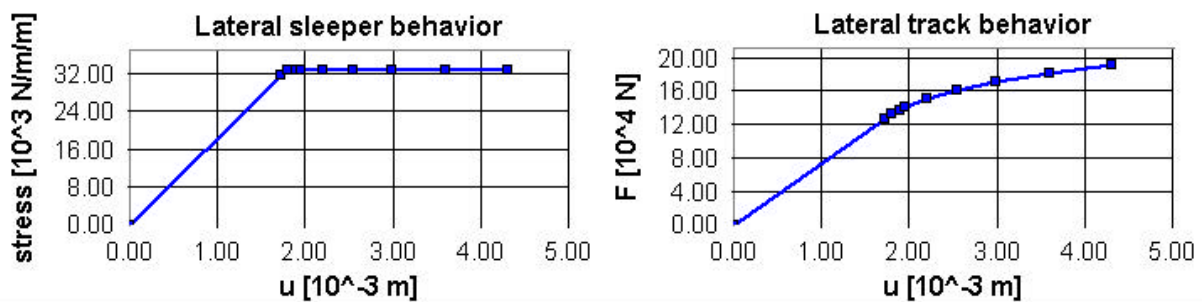


Figure 9 Model obtained using measurement data without vertical load; case with vertical load 100kN

Comparing these results with the experimental data it can be seen that the simulated and measured (average) values of the maximum elastic force, $\bar{F}_p = 132 kN$ in Figure 9 and $\bar{F}_p^{ex} = 132 kN$ in [10] respectively, are very close. From this comparison it can be concluded that the numerical model provides correct results. It should be noticed that the measurement results with extra vertical force can also be used to determine the friction coefficient between the ballast and sleeper.

Determination of speed limits

Now the procedure presented in the previous sections has been applied for determination of speed limits for a track after slipper renewing and tamping of the ballast. The lateral resistance of the track has been measured at different moments after the maintenance [11]. Here three types of measurement data have been used, viz. directly, 3 and 12 days after the maintenance. Using these data ballast elastic limits have been obtained using the parameter identification procedure [8]. They are collected in Table 2. Since the measurement data provide not enough information about plastic behaviour of a track, the parameters characterising plastic behaviour of ballast have been defined based on very conservative assumption that reads

$$F_l = 0.8F_p, \quad W_l = 0.02 m. \quad (15)$$

Using the ballast parameters from Table 2 maximum allowable temperatures have been found for typical train velocities, namely $V = 60, 90, 110, 130, 180 \text{ km/h}$. It should be noted that the set of typical velocities in the software BLATRES can easily be adjusted if other velocities are to be investigated. The maximum allowable temperatures have been determined for a freight train (axle load $F = 225 \text{ kN}$), for a straight track with misalignments $l = 5 \text{ m}$ and $d = 30 \text{ mm}$.

The calculated maximum allowable temperatures are plotted in Figure 10. From this figure it can be seen that lateral resistance of ballast directly after renovation is poor. If the actual equivalent temperature is $T_{equiv} = 40^\circ\text{C}$ as it shown in Figure 9 then the maximum allowable speed of train is $V^* = 60 \text{ km/h}$. The large improvement of ballast quality after 3 days can be explained by the use of stabilisation after the track maintenance.

Measurements	Ballast parameters					
	Fe [N]	We [mm]	Fp [N/m]	Wp [mm]	Fl [N/m]	Wl [mm]
0 days	76500	0.0011	9993	0.17	7994	20
3 days	90260	0.0011	26584	0.35	21267	20
12 days	120030	0.0014	55643	0.69	44514	20

Table 2 Ballast parameters after track renewing [8]

The plots shown in Figure 10 obtained using the procedure described in the paper can be effectively used in assignment of speed limits for renewed tracks.

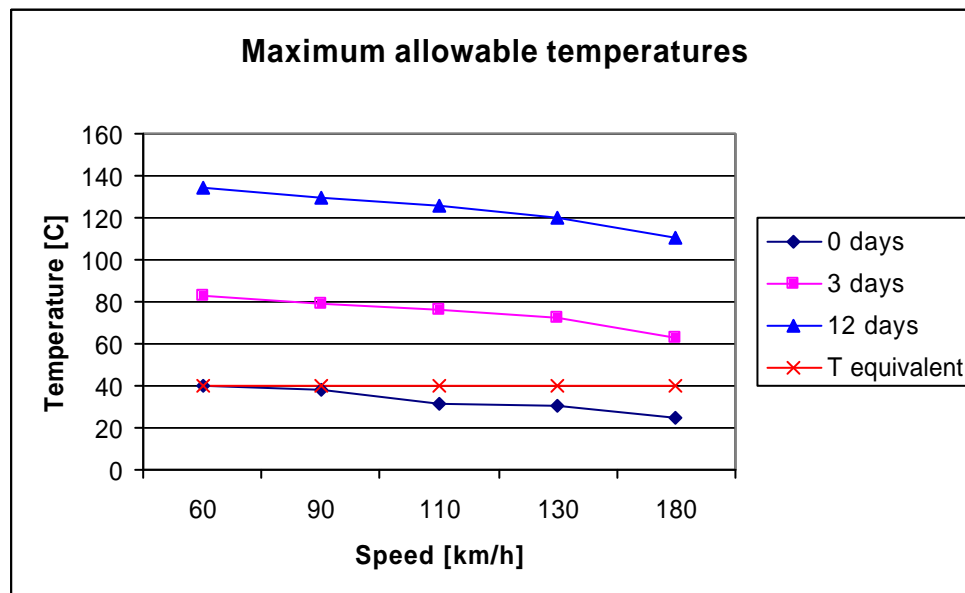


Figure 10 Maximum allowable temperatures for track after renovation

CONCLUSIONS

A procedure for determination of lateral ballast resistance based on measurement result with a real track has been presented. The ballast parameter identification is performed using an optimisation technique. The procedure has been verified using the measurement results with and without extra vertical load.

A technique for determination of speed limits is presented as well. The technique represents a link between measurements of track lateral resistance and UIC safety criteria. It can also provide a ground for assignment of temporary speed limits on tracks after renovation or after full maintenance.

The ballast parameter identification and speed limit determination techniques have been implemented in the software BLATRES that can be installed on existing tamping machines.

REFERENCES

1. CEN (1995) Draft EN BBB-2 - Railway applications - Track Test Methods for Fastening Systems, Part 2, Determination of Torsional Resistance. CEN/TC 256/SC 1/WG 17 N 160, December 1995.
2. ERRI-D202 (1994) Improved Knowledge of Forces in CWR Track (including switches), European Rail Research Institute, ERRI D 202/RP1, Utrecht, August 1994.
3. ERRI-D202 (1995) Improved Knowledge of Forces in CWR Track (including switches), Review of Existing Experimental Work on Behaviour of CWR Track. European Rail Research Institute, ERRI D 202/RP1, Provisional Report, Utrecht, February 1995.
4. ERRI-D202 (1996) Lateral Resistance Test. European Rail Research Institute, Utrecht, ERRI D 202/WG3, Draft Report Deutsche Bahn 50548, September 1996.
5. ERRI-D202 (1996) Lateral Resistance Test. European Rail Research Institute, Utrecht, ERRI D 202/WG3, Draft Report BR research Limited, report RR-TCE-81, November 1996.
6. ERRI-D202 (1996) Laying and Maintenance of CWR Track. International Union of Railways Leaflet 720 R, October 1996.
7. Esveld, C. (1989) *Modern Railway Track*. MRT-Productions, Duisburg. ISBN 90-800324-1-7
8. Markine, V.L., Esveld, C. (1999) Analysis of Lateral Behaviour of a Railway Track Structure Using an Optimization Technique. *Report 7-99-124-1, Laboratory for Road and Railway Engineering, Delft University of Technology*. ISSN 0169-9288
9. Hald, J, Madsen, K. (1985) Combined LP and Quasi-Newton Methods for Nonlinear L1 Optimization. *SIAM J. Numer. Anal.*, Vol. 20, 68-80.
10. NS/CTO (1990) Zijdelingse Weerstandsmetingen van Drie Proefvakken een Referentievak van Elk 300 m op het traject Sittard-Roermond km 22.7-23.9 uitgevoerd in week 44 1989. *Rapport CTO/6/10.256/010*.
11. NS/CTO (1991) Zijdelinkse weerstandsmetingen op het traject Weert-Roermond km 74.430-78.250 uitgevoerd in week 35 van 1990, betreffende een nieuwe werkwijze van dwarsliggers verwisselen met behulp van de Mechanische Dwarsligger Verwisseling (MDV). *Rapport CTO/6/10.473/0005*

12. Samavedam, G., Kish, A., Purple, A., Schoengart, J. (1993) Parametric Analysis and Safety Concepts of CWR Buckling, U.S. Department of Transportation, John A. Volpe National transportation Systems Center, Cambridge. *Report DOT-VNTSC-FRA-93-25*, December 1993.
13. Samavedam, G. (1995) *Theory of CWR Track Stability*. Foster-Miller, Inc. Walthman.
14. Van, M.A. (1997) Stability of Continuous Welded Rail Track. Ph.D. Thesis, Delft University Press. ISBN 90-407-1485-1
15. Zand, J. van 't and Moraal, J. (1997) Ballast Resistance under Three Dimensional Loading. Delft University of Technology, Faculty of Civil Engineering, Laboratory of Roads and Railways, report 7-97-103-4, February 1997.